Available online at www.sciencedirect.com
ScienceDirect
International Journal of Mass Spectrometry 266 (2007) 122–128
International Journal of Mass Spectrometry
www.elsevier.com/locate/ijms

Potential crossing position in electron transfer of a doubly charged ion and an alkali metal target measured using thermometer molecule $W(CO)_6$

Shigeo Hayakawa [a,*], Kaori Minami [a], Kenichi Iwamoto [a], Michisato Toyoda [b], Toshio Ichihara [b], Hirofumi Nagao [c]

[a] *Department of Chemistry, Graduate School of Science, Osaka Prefecture University, 1-1 Gakuencho, Nakaku, Sakai, Osaka 599-8531, Japan*
[b] *Department of Physics, Graduate School of Science, Osaka University, 1-1 Machikaneyama, Toyonaka, Osaka 560-0043, Japan*
[c] *Division of Sustainable Energy and Environmental Engineering, Graduate School of Engineering, Osaka University, 2-1 Yamadaoka, Suita, Osaka 565-0871, Japan*

Received 3 May 2007; received in revised form 23 July 2007; accepted 23 July 2007
Available online 28 July 2007

Abstract

Doubly charged tungsten hexacarbonyl $W(CO)_6^{2+}$ ions were made to collide with K and Cs targets to give singly and doubly charged positive ions by collision-induced dissociation (CID). The internal energy depositions resulting from the electron transfer were evaluated from the relative abundances of the singly charged fragment $W(CO)_n^+$ ions. The internal energy deposition resulting from the electron transfer with the Cs target was very narrow and centered at a particular energy, 8.2 eV above the energy level of the charge reduced $W(CO)_6^+$ ion, which was higher than 7.2 eV with the K target. These internal energies correspond to energy differences of 2.9 and 3.5 eV between the entrance channel of $W(CO)_6^{2+} + Cs$ (or K) and the exit channel of $W(CO)_6^{+*} + Cs^+$ (or K^+), respectively. The potential energy between $W(CO)_6^{2+}$ ions and the alkali metal atoms was found to decrease markedly in the entrance channel of the electron transfer as a result of the large polarizability of the alkali metal targets. The internuclear separation of the Landau–Zener potential crossing of the electron transfer between a $W(CO)_6^{2+}$ ion and the Cs target was evaluated as 6.8×10^{-8} cm, which was larger than the value for the K target (5.9×10^{-8} cm). Large cross sections for the electron transfer of the order of 10^{-14} cm^2, estimated from the internuclear distances, indicate that the electron capture of the doubly charged ion on collisions with an alkali metal targets is a very effective process for producing charge-reduced ions. The difference in the cross sections between K and Cs target indicates that a target having lower ionization energy is more effective for electron transfer.

Keywords: Electron transfer dissociation (ETD); Internal energy distribution; Thermometer molecule; Potential crossing; Collision-induced dissociation (CID)

1. Introduction

Since the development of electrospray ionization [1], there has been a growing interest in electron capture and electron transfer processes of multiply charged ions formed from large biomolecules as electron capture dissociation (ECD) [2–5] or electron transfer dissociation (ETD) [6,7]. These processes have been studied to obtain information about the dissociation of molecular projectile ions, particularly amino acid sequences in peptides and proteins. The usefulness of the electron capture and electron transfer process is associated with N–Cα bond cleavages to form c- and z-type ions [8,9] without the loss of labile posttranslational modification groups [2–7]. The mechanism of N–Cα bond cleavage reactions has been studied by Turecek and coworkers [10–13]. N–Cα bond cleavages induced by electron transfer processes of multiply charge peptides on collision with neutral targets, such as alkali metals [14,15], or metastable rare gases [16] have also been reported. Because the dissociation behavior of isolated molecules is controlled by the internal energy distribution $P(\varepsilon)$ of the molecular population, it is of fundamental importance to be able to characterize this distribution for charged ions whose charge is reduced by electron transfer. The current interest in ECD and ETD of multiply charged ions of large biomolecules also makes it important to develop methods

* Corresponding author.
E-mail address: hayakawa@c.s.osakafu-u.ac.jp (S. Hayakawa).

1387-3806/$ – see front matter © 2007 Elsevier B.V. All rights reserved.
doi:10.1016/j.ijms.2007.07.015

for characterizing their internal energy distributions. Theoretical calculations to estimate the internal energy and the cross section are virtually impossible for electron transfer processes involving multiply charged ions of large biomolecules, because of the multitude of ion structures and dissociation pathways involved.

Beynon and coworkers [17–19] reported an approximate thermometer method in which branching ratios were used to characterize energy deposition associated with photodissociation. Wysocki et al. [20] have reported the use of so-called thermometer molecules to measure internal energy distributions $P(\varepsilon)$ of gas-phase ions. By using the same method, Cooks and coworkers determined the internal energy distributions, $P(\varepsilon)$, in doubly charged ions following electron transfer in high-energy collisions by using a sector-type mass spectrometer and in low-energy collisions by using a triple quadrupole mass spectrometer with various atomic and molecular targets [21–23]. One of the authors have previously measured the internal energy distribution of neutral species formed through neutralization in charge-inversion mass spectrometry with alkali metal targets by using the thermometer molecule $W(CO)_6$ [24]. The internal energy distributions in the charge-inversion mass spectrometry indicated that dissociation occurs in the energy-selected neutral species formed by way of near-resonant neutralization [24–26]. We recently reported differences between the internal energy depositions induced by collisional activation and by electron transfer of $W(CO)_6^{2+}$ ions on collision with Ar and K targets [27]. The internal energy deposition in collisionally activated dissociation (CAD) evaluated with the Ar target was broad and decreased with increasing internal energy. On the contrary to this, internal energy deposition evaluated with the K target was very narrow and centered at a particular energy, 7.8 eV below the energy level of the $W(CO)_6^{2+}$ ion. This narrow internal energy distribution was explained in terms of electron transfer by Landau–Zener [28–30] potential crossing at a separation of 5.9×10^{-8} cm between a $W(CO)_6^{2+}$ ion and a K atom, and the coulombic repulsion between singly charged ions in the exit channel. These results were compared with a classical overbarrier model [31,32], that successfully explained processes involving electron capture by multiply charged atomic ions in collision with atoms or simple molecules. From these experimental results, we proposed that the terms "CID" and "CAD", which were similarly defined [33], should not be used interchangeably, on the basis that there are differences in the observed ions and in their intensities with Ar and K targets.

In the present work, we measured the collision-induced dissociation (CID) spectra of doubly charged $W(CO)_6^{2+}$ ions following collision with either an K target or a Cs target. While the internal energy distributions obtained with both the K and Cs targets were very narrow, the average internal energy with a K target was lower than that with a Cs target. From the similarities and differences between the K and Cs target, we concluded that electron transfer from the alkali metal proceeds through a potential crossing at a large internuclear distance and that polarizability of the target is an important factor determining the position of the potential crossing.

2. Experimental

Mass-selected doubly charged ions were made to collide with alkali metal targets, and the resulting singly and doubly charged ions that formed upon electron transfer and collisional activation were mass analyzed by using an MS/MS instrument [27]. An extensive description of the apparatus used in this work has been presented in the previous paper. Only a brief description and pertinent points to the present work will be given here. Doubly charged $W(CO)_6^{2+}$ ions were formed by 70 eV electron ionization and accelerated to a kinetic energy of 10 keV by an accelerating voltage of 5 kV. The precursor ions were mass selected by a JEOL JMS-HX110 double-focusing mass spectrometer (MS-I). The mass-selected precursor ions entered a 3.7 cm long collision cell located at the exit of MS-I. The alkali metal targets were introduced into the collision cell as a vapor from a reservoir through a ball valve. The singly and doubly charged positive ions were mass-analyzed by a spherical electrostatic analyzer having a 216 mm central radius (MS-II). The mass-analyzed ions were detected by a 9 kV post-acceleration secondary-electron multiplier. The vacuum chamber mounting the collision cell evacuated by Seiko STP-300H turbo molecular pumps and MS-II were differentially evacuated by Balzers Pfeiffer TMH-260 turbo molecular pumps. The pressures measured by ionization gauges mounted on both the vacuum chamber and on MS-II were less than 6×10^{-5} Pa when the target gas was not supplied.

CID spectra were measured by mass-analyzing the singly and doubly charged positive ions leaving the collision cell by scanning the electric field in MS-II from 0 to twice the electric field that causes the primary doubly charged ions to pass through the MS-II. The temperatures of the collision cell, the ball valve, and the reservoir were adjusted to control the density of alkali metal in the collision cell. Tungsten hexacarbonyl [$W(CO)_6$; 99%, Aldrich, USA)] was used as received.

3. Results and discussion

The CID spectra of the doubly charged tungsten hexacarbonyl cation $W(CO)_6^{2+}$ with K and Cs as the targets are shown in Fig. 1(a and b). Singly charged fragment ions were formed by electron transfer followed by dissociation, and doubly charged fragment ions were formed by collisional activation (CA), as shown in the previous paper [27]. In the both CID spectra, the non-dissociated $W(CO)_6^{2+}$ peak at $m/z = 176$ is by far the strongest, with a height higher than the upper limit of the scale of the vertical axis. The high intensity of this $W(CO)_6^{2+}$ peak was attributed to a precursor ion that does not interact with the target. In the CID spectrum with both K [Fig. 1(a)] and Cs [Fig. 1(b)] targets, the predominant peaks at $m/z = 240$ and 268 are associated with singly charged $W(CO)_2^+$ and $W(CO)_3^+$ ions, respectively. The singly charged fragment $W(CO)_2^+$ and $W(CO)_3^+$ ions result from electron transfer followed by a loss of four and three CO ligands, respectively. The relative abundances of these two peaks are much different between the K and Cs targets. The relative abundance of the peak associated with $W(CO)_2^+$ ions compared with that for $W(CO)_3^+$ ions is 1.0:1.66 with K target in

Table 1
The relative abundances of $W(CO)_n^{2+}$ ($n = 1$–5) and $W(CO)_m^{+}$ ($m = 1$–6) obtained from the CID spectra

Singly charged ions			Doubly charged ions		
Ion	Target		Ion	Target	
	K	Cs		K	Cs
$W(CO)_6^{+}$	–	–	$W(CO)_6^{2+}$		
$W(CO)_5^{+}$	–	–	$W(CO)_5^{2+}$	3	3
$W(CO)_4^{+}$	2	–	$W(CO)_4^{2+}$	1	–
$W(CO)_3^{+}$	100	49	$W(CO)_3^{2+}$	–	–
$W(CO)_2^{+}$	63	100	$W(CO)_2^{2+}$	–	–
$W(CO)^{+}$	8	7	$W(CO)^{2+}$	–	–
W^{+}	4	5	W^{2+}	–	–

The abundances are normalized to that of the largest fragment peak associated with the $W(CO)_3^{+}$ and $W(CO)_2^{+}$ ions with K and Cs targets, respectively. The relative abundances are evaluated from the average of the several mass spectra measured in different target pressures under the single-collision conditions. Intensities lower than 1% are shown as "–".

Fig. 1(a) and 1.0:0.49 with the Cs target in Fig. 1(b). The relative abundances associated with $W(CO)^{+}$ ($m/z = 212$) and $W(CO)_2^{+}$ ($m/z = 240$) ions in the Cs target [Fig. 1(b)] are higher than those in the K target [Fig. 1(a)]. The higher intensity of the lower mass ions with the Cs target than that with the K target indicates that the internal energy of the charge-reduced $W(CO)_6^{+*}$ ions obtained on collisions with the Cs target was higher than that with the K target. The very weak peaks associated with doubly charged $W(CO)_m^{2+}$ ($m = 4$, 5) ions resulting from cleavage of the W–CO bonds are observed at $m/z = 148$ and 162 in both spectra of Fig. 1. The relative abundances of $W(CO)_n^{2+}$ ($n = 4$, 5) and $W(CO)_n^{+}$ ($n = 1$–6) obtained from the CID spectra following collisions with K and Cs targets are shown in Table 1; the relative abundances are evaluated from the average of several CID spectra measured at different target pressures under the single-collision conditions. The peak intensities of the doubly charged fragment ions are much lower than those associated with singly charged $W(CO)_m^{+}$ ($m = 2$, 3) ions. The excessive intensity difference between the singly charged ions and doubly charged ions indicated that the electron transfer process was much effective than CA in the case of collisions with alkali metal targets. This result is explained by the fact that the difference in the cross section of the electron transfer of doubly charged ions on collision with the alkali metal targets, which is of the order of 10^{-14} cm^2 is much larger than that of CA, which is of the order of 10^{-16} cm^2 [27].

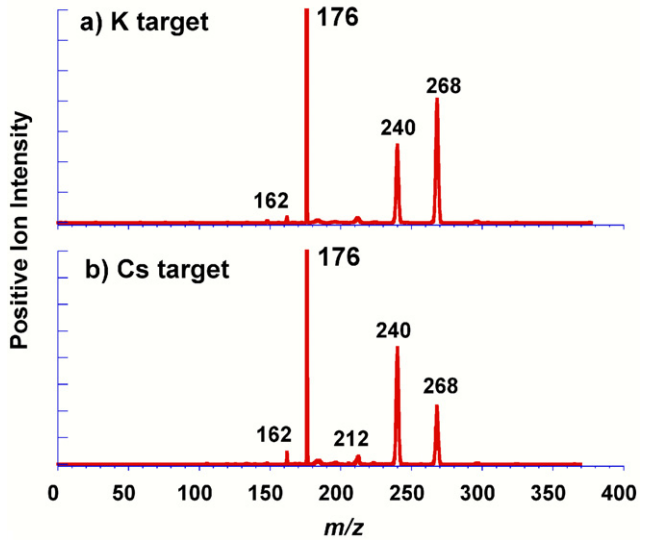

Fig. 1. Collision-induced dissociation (CID) spectra of the doubly charged tungsten hexacarbonyl cation [$W(CO)_6^{2+}$] with K and Cs as targets. The target gas is K for (a) and Cs for (b). The scales on the vertical axes of the spectra in (a) and (b) are normalized at the intensities of the strongest fragment peaks in the respective spectra, which are associated with the $W(CO)_3^{+}$ ions and $W(CO)_2^{+}$ ions, respectively.

The method to evaluate the internal energy distribution $P(\varepsilon)$ was reported by Wysocki et al. [20] by using the peak abundances in the spectra and the thermochemical data. The thermochemical data for $W(CO)_6^{+}$, $W(CO)_6^{2+}$, and their fragment ions are listed in Table 2. The thermochemical data of IE/AE values for singly charged ions and for doubly charged ions are reported by Wysocki et al. and Cooks et al., which were obtained from the measured ionization energy of the $W(CO)_6^{+}$ ion and the appearance energies of the fragment ions [20,21]. This method assumed that all the ions that have enough internal energy to dissociate do so and that they undergo the most endothermic reaction open to them. All the charge reduced $W(CO)_6^{+*}$ ions with energies between the activation energies for formation of $W(CO)_m^{+}$ ions and $W(CO)_{m-1}^{+}$ ions [$\Delta E(m)$ and $\Delta E(m-1)$, respectively] are assumed to fragment to yield $W(CO)_m^{+}$ ions. The relative abundance of each fragment $W(CO)_m^{+}$ ion is taken as a measure of the number of charge reduced $W(CO)_6^{+*}$ ions with internal energies between $\Delta E(m)$ and $\Delta E(m-1)$. The abundances of fragment $W(CO)_m^{+}$ ions divided by the energy range $\Delta E(m-1) - \Delta E(m)$ gives the data height in $P(\varepsilon)$ between $\Delta E(m)$ and $\Delta E(m-1)$, which allow a comparison to be made between the relative abundances in $P(\varepsilon)$ and those in the CID spectra. To apply the method in the present work, some other additional assumptions are necessary, including the following: (1) a low initial energy of the parent $W(CO)_6^{2+}$ ions; (2) a low translational energy in the center of mass system of fragments after dissociation; (3) a low internal energy in fragment CO molecules; and (4) the short dissociation lifetimes of $W(CO)_m^{+}$ ions. These assumptions (1)–(4) were rationalized in the previous paper [27].

Table 2
Thermochemical data for $W(CO)_6^+$, $W(CO)_6^{2+}$, and their fragment ions

Singly charged ions				Doubly charged ions			
Ion	IE/AE	BE	ΔE	Ion	IE/AE	BE	ΔE
$W(CO)_6^+$	8.5		0.0	$W(CO)_6^{2+}$	23.5		15.0
$W(CO)_5^+$	9.7	1.2	1.2	$W(CO)_5^{2+}$	24.5	1.0	16.0
$W(CO)_4^+$	11.9	2.2	3.4	$W(CO)_4^{2+}$	27.3	2.8	18.8
$W(CO)_3^+$	13.7	1.8	5.2	$W(CO)_3^{2+}$	29.7	2.4	21.2
$W(CO)_2^+$	16.0	2.3	7.5	$W(CO)_2^{2+}$	32.0	2.3	23.5
$W(CO)^+$	18.6	2.6	10.1	$W(CO)^{2+}$	35.7	3.7	27.2
W^+	21.5	2.9	13.0	W^{2+}	38.6	2.9	30.1

IE/AE are the ionization energies or appearance energies and BE are the bond energies. ΔE are energy differences from the energy level of the charge reduced $W(CO)_6^+$ ion. All values are in eV. IE/AE values for singly charged ions are taken from Wysocki et al. [20]. IE/AE values for doubly charged ions are taken from Cooks et al. [21].

Fig. 2(a and b) shows the internal energy distributions, $P(\varepsilon)$, obtained from the relative abundances tabulated in Table 1 evaluated from the CID spectra with the K and Cs targets and by using the thermochemical data tabulated in Table 2, by using the same method as that reported by Wysocki et al. [20] The internal energies are scaled from the energy level of the charge reduced $W(CO)_6^+$ ion. In Fig. 2(a and b), the $P(\varepsilon)$ values between 5.2 and 7.5 eV correspond to the abundances of the peaks associated with the $W(CO)_3^+$ ion in Fig. 1(a and b), whereas those between 7.5 and 10.1 eV correspond to those associated with the $W(CO)_2^+$ ion. The peak associated with the precursor $W(CO)_6^{2+}$ ion contains the contributions that did not interact with the target, and the relative intensity of this peak relative to those of the fragment ions depends on the target density. Therefore, the value between 15.0 and 16.0 eV that corresponds to the intensity of the precursor $W(CO)_6^{2+}$ ion is not plotted. The values that correspond to the intensities of the atomic singly charged W^+ ions are not plotted, because the upper limits of the internal energies are not determined for atomic ions.

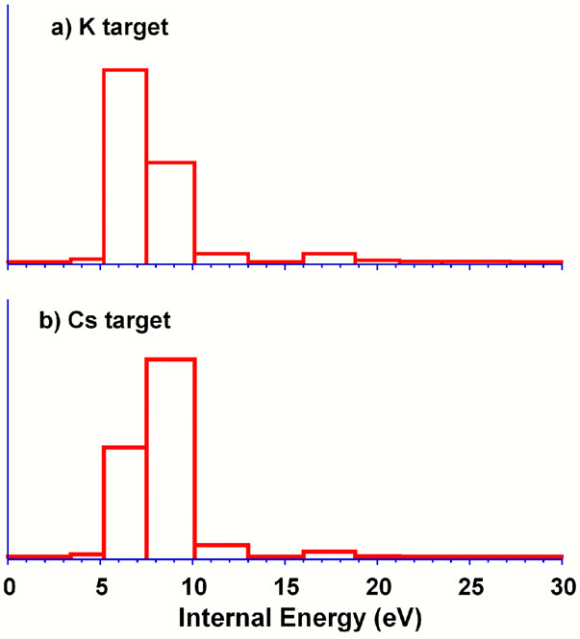

Fig. 2. Internal energy distributions, $P(\varepsilon)$, obtained from the relative abundances listed in Table 1 and evaluated from the CID spectra with the K (a) and Cs (b) targets and calculated by using the thermochemical data reported by Wysocki et al. [20] and from Cooks et al. [21] The scales on the vertical axes of $P(\varepsilon)$ distributions for the K (a) and Cs targets (b) are normalized at the height of the strongest fragments in the respective spectra, which are associated with $W(CO)_3^+$ ions and $W(CO)_2^+$ ions, respectively.

As Fig. 2 show the relative abundances, the plots for the K target in Fig. 2(a) and for the Cs target in Fig. 2(b) are normalized at the largest $P(\varepsilon)$ value between 5.2 and 7.5 eV and to that between 7.5 and 10.1 eV, respectively. The intensity of the singly charged ions formed by electron transfer is much larger than that in the positive region of the doubly charged fragment ions formed from collisional activation for both K and Cs target. This intensity difference indicates that the relative cross section for electron transfer is much larger than that for collisional activation with alkali metal targets. The presence of the narrow maximum peak in the internal energy distribution for the singly charged ions formed by electron transfer from the K and Cs targets shows that a specific excitation for the singly charged $W(CO)_6^{+*}$ formed by the electron transfer predominates in the case of alkali metal targets, as is the case in charge-inversion mass spectrometry [24–26]. The internal energy distribution for the Cs target is higher than that for the K target, as shown in Fig. 2. The average internal energy for the K target, evaluated from the relative abundances of the $W(CO)_2^+$ ion and the $W(CO)_3^+$ ion, is 7.2 eV. As the fragment ions with the maximum intensity were $W(CO)_2^+$ ions in the case of the Cs target, the average value of the internal energy for the Cs target was evaluated to be 8.2 eV from the abundances of $W(CO)^+$ to $W(CO)_3^+$ ions. The lower values of the average internal energy for both targets than the energy level of 15 eV for the precursor $W(CO)_6^{2+}$ ion indicated that the electron transfer on collision with alkali metal targets provided the charge reduced $W(CO)_6^{+*}$ whose energy was lower than the precursor $W(CO)_6^{2+}$ ion. The internal energy distributions for the K target, in which the energies were scaled from the energy level of the precursor $W(CO)_6^{2+}$ ion, was already shown in the previous paper [27]. The average internal energy of 7.2 eV scaled from the energy level of the charge reduced $W(CO)_6^+$ ion is identical to that of −7.8 eV scaled from the energy level of the precursor $W(CO)_6^{2+}$ ion.

Energy levels of $W(CO)_6^+$, $W(CO)_6^{2+}$, and their fragment ions are shown in Fig. 3. The energy values of the fragments are scaled from the ground state of the charge reduced $W(CO)_6^+$

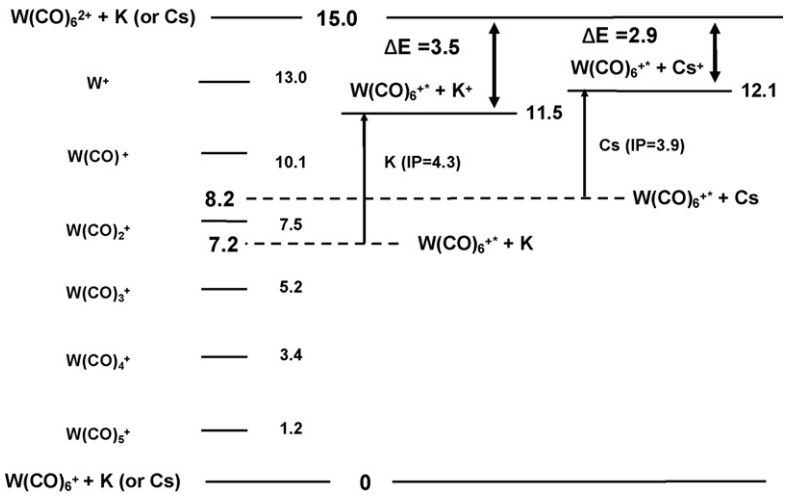

Fig. 3. Energy levels of $W(CO)_6^+$, $W(CO)_6^{2+}$, and their fragment ions in electron volts. The thermochemical data are from Wysocki et al. [20] and from Cooks et al. [21] The average values of the internal energy of $W(CO)_6^{+*}$ were evaluated from the data shown in Fig. 2. For the sake of clarity, K and Cs are omitted from the energy levels of the fragments. The energy differences between the entrance channel of $W(CO)_6^{2+} + K$ (or Cs) and the exit channels of $W(CO)_6^{+*} + K^+$ (or Cs^+) were evaluated to be 3.5 and 2.9 eV, respectively.

and a neutral alkali metal, whose energy is 15 eV lower than the entrance channel of the collision. The average energy level of $W(CO)_6^{+*}$ ions for K and Cs targets estimated from the internal energy distribution for the electron transfer process in Fig. 2 are 7.2 and 8.2 eV, respectively. The energy level of 7.2 (or 8.2) eV corresponds to an energy level of the $W(CO)_6^{+*} + K$ (or Cs) reaction. The energy level of the exit channel of $W(CO)_6^{+*} + K^+$ (or Cs^+) in the reaction of the present work is higher than that of $W(CO)_6^{+*} + K$ (or Cs) by an amount equal to the ionization energy of the respective target. Since the ionization energies of K and Cs are 4.34 and 3.89 eV, respectively, the energy differences of 3.5 and 2.9 eV are evaluated to be those between the entrance channel of $W(CO)_6^{2+} + K$ (or Cs) and the exit channel of $W(CO)_6^{+*} + K^+$ (or Cs^+). While the electron transfer process between singly charged ions and an alkali metal target was near-resonant as demonstrated by our group [24–26], the energy differences of 3.5 and 2.9 eV indicated that the electron transfer between the doubly charged ions and the alkali metal targets were not near-resonant process. These differences have been explained in terms of an ion-induced dipole in the entrance channel and a coulomic repulsion in the exit channel as discussed in the previous paper [27]. The process most likely to be responsible for electron transfer is Landau–Zener curve crossing [28–30], which is represented schematically in Fig. 4. In this model, the doubly charged ion and the target gas approach each other along an ion-induced dipole curve; at some critical distance (R_c), electron transfer takes place and the two singly charged positive ions exit on a coulombic repulsion curve. The energy difference (ΔE) of this process between the entrance and the exit channels is calculated by using Eq. (1),

$$\Delta E = \frac{e^2}{4\pi\varepsilon_0 R_c} + \frac{\alpha(2e)^2}{32\pi^2\varepsilon_0^2 R_c^4} \quad (1)$$

where e is the electric charge, ε_0 is the permittivity of a vacuum, and α represents the polarizability of the target. The Landau–Zener curve crossing near the critical distance of the electron transfer is represented schematically in Fig. 4. The energy levels of the entrance channel decrease with decreasing the internuclear distance, because of the large polarizabilities for the K and Cs targets, whose values are 43.4×10^{-30} and 59.6×10^{-30} m^3 [34,35], respectively. Based on the energy difference between the entrance and exit channels evaluated from the maximum in the internal-energy distribution, an critical distances of the electron transfer of $W(CO)_6^{2+}$ and K and Cs targets are evaluated to be 5.88×10^{-8} and 6.83×10^{-8} cm, respectively. This potential crossing at this large internuclear distance meets the criterion for electron transfer by the Landau–Zener curve crossing. The decrease in the energy as a result of the ion-induced dipole in the entrance channel at the critical points from the infinite internuclear distance are 1.05 eV for the K target and 0.79 eV for the Cs target. The ratio between the decreases in the energy and the energy differences between the entrance

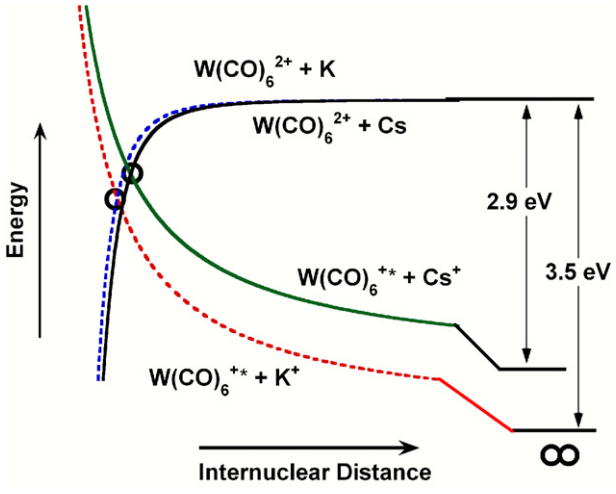

Fig. 4. Schematic of the potential energy curves near the critical distance of Landau–Zener [28–30] potential crossing. The ◯ symbols indicate positions of the potential crossing of respective targets.

and the exit channel for the K and the Cs targets are 30 and 27%, respectively. If these decreases are neglected, the critical distances for the K and Cs targets become 4.11×10^{-8} and 4.96×10^{-8} cm, respectively. The decrease of more than 27% in the energy and the difference in the critical distances indicate that the decrease in the energy as a result of the ion-induced dipole cannot be neglected in evaluating the critical distance of electron transfer in case using alkali metal targets. The critical distances estimated in this work are longer than the internuclear distances of the alkali metal molecules K_2 and Cs_2 reported to be 3.91×10^{-8} and 4.47×10^{-8} cm, respectively [36]. Electronic structures of the alkali metal molecules were well represented by two valence s electrons with well-separated inner cores [37]. Whereas the ratio of the estimated critical distances between K and Cs is 0.86, the ratio of the internuclear distances of the diatomic molecules is 0.87. The larger values of the critical distance compared with the internuclear distances of the molecules and the similarity of their ratios suggests that electron transfer between doubly charged ions and an alkali metal target takes place from the outmost s orbital.

While the cross section estimated on the basis of an internuclear distance of 5.88×10^{-8} cm for K target is 1.09×10^{-14} cm^2, that of 6.83×10^{-8} cm for Cs target is 1.47×10^{-14} cm^2. The cross section of the order of 10^{-14} cm^2 estimated in the present work is much larger than that for collisional activation, which has been estimated to be in order of 10^{-16} cm^2 [27,38]. We believe that the electron transfer processes of multiply charged ions of large biomolecules that follow collision with alkali metal targets will provide information about the dissociation of molecular projectile ions, particularly about amino-acid sequences in peptides and proteins, in the same manner as do the isomeric differentiations in charge-inversion mass spectrometry [27,38–41].

4. Conclusion

The intensity distribution of the fragment ions in the collision-induced dissociation (CID) spectra of doubly charged $W(CO)_6^{2+}$ ions on collision with alkali metal targets indicated that the major process in CID is dissociation of charge reduced singly charged ions formed by electron transfer. From thermochemical considerations based on the relative abundance of the fragment charge reduced $W(CO)_n^+$ ions, the average internal energy of the temporal $W(CO)_6^{+*}$ ions formed by electron transfer on collision with the K and Cs target was estimated to be 7.2 and 8.2 eV above the energy level of the charge reduced $W(CO)_6^+$ ions, respectively. On the basis of energy differences of 3.5 and 2.9 eV between the entrance channel and the exit channels of the electron transfer process, the internuclear distances at the potential crossing for the K and Cs targets were estimated to be 5.88×10^{-8} and 6.83×10^{-8} cm, respectively. As the decrease in the energy in the entrance channel caused by the ion-induced dipole for the K and Cs targets were 30 and 27%, respectively, of the energy difference between the entrance and exit channels, the decrease in the energy cannot be neglected in evaluating the internuclear distance of electron transfer when alkali metal targets (which have large polarizabilities) are used. The electron transfer cross sections for the K and Cs targets were estimated to be 1.09×10^{-14} and 1.47×10^{-14} cm^2, respectively. On the basis of these large cross sections for the electron transfer (of the order of 10^{-14} cm^2), we suggest that alkali metal are very effective targets for producing charge reduced ions from doubly charged peptide ions.

Acknowledgements

This work was supported by Special Research Grant from Osaka Prefecture University, 2007. The authors express their appreciation to Dr. M. Ishihara and H. Adachi at Osaka University for their help with the experiments.

References

[1] J.B. Fenn, M. Mann, C.K. Meng, S.F. Wong, C.M. Whitehouse, Science 246 (1989) 64.
[2] R.A. Zubarev, N.L. Kelleher, F.W. McLafferty, J. Am. Chem. Soc. 120 (1998) 3265.
[3] R.A. Zubarev, N.A. Kruger, E.K. Fridriksson, M.A. Lewis, D.M. Horn, B.K. Carpenter, F.W. McLafferty, J. Am. Chem. Soc. 121 (1999) 2857.
[4] R.A. Zubarev, K.F. Haselmann, B. Budnik, F. Kjeldsen, F. Jensen, Eur. J. Mass Spectrom. 8 (2002) 337.
[5] R.A. Zubarev, Mass Spectrom. Rev. 22 (2003) 57.
[6] J.E.P. Syka, J.J. Coon, M.J. Schroeder, J. Shabanowitz, D.F. Hunt, Proc. Natl. Acad. Sci. U.S.A. 101 (2004) 9528.
[7] J.J. Coon, J.E.P. Syka, J.C. Schwartz, J. Shabanowitz, D.F. Hunt, Int. J. Mass Spectrom. 236 (2004) 33.
[8] P. Roepstorff, J. Fohlman, Biomed. Mass Spectrom. 11 (1984) 601.
[9] K. Biemann, Biomed. Environ. Mass Spectrom. 16 (1988) 99.
[10] F. Turecek, J. Am. Chem. Soc. 125 (2003) 5954.
[11] F. Turecek, E.A. Syrstad, J. Am. Chem. Soc. 125 (2003) 3353.
[12] E.A. Syrstad, F. Turecek, J. Am. Soc. Mass Spectrom. 16 (2005) 208.
[13] X.H. Chen, F. Turecek, J. Am. Chem. Soc. 128 (2006) 12520.
[14] P. Hvelplund, B. Liu, S.B. Nielsen, S. Tomita, Int. J. Mass Spectrom. 225 (2003) 83.
[15] T. Chakraborty, A.I.S. Holm, P. Hvelplund, S.B. Nielsen, J.C. Poully, E.S. Worm, E.R. Williams, J. Am. Soc. Mass Spectrom. 17 (2006) 1675.
[16] V.D. Berkout, Anal. Chem. 78 (2006) 3055.
[17] E.S. Mukhtar, I.W. Griffiths, F.M. Harris, J.H. Beynon, Int. J. Mass Spectom. Ion Phys. 37 (1981) 159.
[18] I.W. Griffiths, E.S. Mukhtar, R.E. March, F.M. Harris, J.H. Beynon, Int. J. Mass Spectom. Ion Phys. 39 (1981) 125.
[19] I.W. Griffiths, E.S. Mukhtar, F.M. Harris, J.H. Beynon, Int. J. Mass Spectom. Ion Phys. 43 (1982) 283.
[20] V.H. Wysocki, H.I. Kenttamaa, R.G. Cooks, Int. J. Mass Spectom. Ion Process. 75 (1987) 181.
[21] R.G. Cooks, T. Ast, B. Kralj, V. Kramer, D. Zigon, J. Am. Soc. Mass Spectrom. 1 (1990) 16.
[22] L.E. Dejarme, R.G. Cooks, T. Ast, Org. Mass Spectrom. 27 (1992) 667.
[23] R. Susic, L. Lu, D.E. Riederer, D. Zigon, R.G. Cooks, T. Ast, Org. Mass Spectrom. 27 (1992) 769.
[24] S. Hayakawa, K. Harada, K. Arakawa, N. Morishita, J. Chem. Phys. 112 (2000) 8432.
[25] S. Hayakawa, K. Harada, N. Watanabe, K. Arakawa, N. Morishita, Int. J. Mass Spectrom. 202 (2000) A1.
[26] S. Hayakawa, Int. J. Mass Spectrom. 212 (2001) 229.
[27] S. Hayakawa, A. Kitaguchi, S. Kameoka, M. Toyoda, T. Ichihara, J. Chem. Phys. 124 (2006) 224320.
[28] L. Landau, Z. Phys. Sowiet 2 (1932) 46.

[29] E.C.G. Stuecklberg, Helv. Phys. Acta 5 (1932) 370.
[30] C. Zener, Proc. R. Soc. A 137 (1932) 696.
[31] H. Ryufuku, K. Sasaki, T. Watanabe, Phys. Rev. A 21 (1981) 745.
[32] A. Barany, G. Astner, H. Cederquist, H. Danared, S. Huldt, P. Hvelplund, A. Johnson, H. Knudsen, L. Liljeby, K.G. Rensfelt, Nucl. Instrum. Methods Phys. Res. B 9 (1985) 397.
[33] J.F.J. Todd, Int. J. Mass Spectom. Ion Process. 142 (1995) 209.
[34] T.M. Miller, B. Bederson, Adv. At. Mol. Phys. 13 (1977) 1.
[35] T.M. Miller, B. Bederson, Adv. At. Mol. Phys. 25 (1988) 37.
[36] K.P. Huber, G. Herzberg, Molecular Spectra and Molecular Structure IV. Constants of Diatomic Molecules, vol. IV, Van Nostrand Reinhold, New York, 1979.
[37] W. Muller, W. Meyer, J. Chem. Phys. 80 (1984) 3311.
[38] S. Hayakawa, J. Mass Spectrom. 39 (2004) 111.
[39] S. Hayakawa, Y. Kawamura, Y. Takahashi, Int. J. Mass Spectrom. 246 (2005) 56.
[40] S. Hayakawa, A. Kitaguchi, J. Mass Spectrom. 41 (2006) 1226.
[41] S. Hayakawa, N. Kabuki, Eur. Phys. J. D 38 (2006) 163.